

Transient Simulation of Graphene Sheets using a Deterministic Boltzmann Equation Solver

Sung-Min Hong

Abstract—Transient simulation capability with an implicit time derivation method is a missing feature in deterministic Boltzmann equation solvers. The H-transformation, which is critical for the stable simulation of nanoscale devices, introduces difficulties for the transient simulation. In this work, the transient simulation of graphene sheets is reported. It is shown that simulation of homogeneous systems can be done without abandoning the H-transformation, as much as a specially designed discretization method is employed. The AC mobility and step response of the graphene sheet on the SiO₂ substrate are simulated.

Index Terms—Transient simulation, deterministic Boltzmann equation solver, Boltzmann transport equation, graphene

I. INTRODUCTION

The Boltzmann transport equation plays a central role in the semi-classical transport theory. Since deterministic Boltzmann equation solvers have many advantages over the conventional Monte Carlo method, they have gained research interest recently [1]. In addition to the steady-state analysis, small-signal [1, 2] and noise [3, 4] analyses are also possible.

However, compared to the traditional drift-diffusion-based device simulators, an important simulation feature – the transient simulation capability – is seldom exploited in the deterministic Boltzmann solvers [5]. It

restricts application area of the deterministic Boltzmann solver significantly. For example, the plasma instability in the quasi-ballistic transistor channel [6, 7] requires an accurate device solver with the transient capability.

Although the transient simulation of the double-gate MOSFET using a deterministic Boltzmann equation solver has been reported recently [8], a special time-marching scheme is adopted. Other attempts for solving the transient Boltzmann transport equation using deterministic solvers [9, 10] adopt WENO (Weighted Essentially Non-Oscillatory) scheme, whose time-marching scheme is much different from the implicit time derivation method, typically used in the conventional device simulators.

In this work, our recent effort to develop a deterministic Boltzmann equation solver with the transient simulation capability is presented. In addition to the conference presentation [11], actual simulation results are added. Due to its high carrier mobility and large saturation velocity, graphene has been considered as a very promising candidate for high-frequency devices [12]. However, simulation of graphene devices with the conventional drift-diffusion model [13] is highly nontrivial because of the unique band structure. In this sense, graphene devices are good model systems to test the Boltzmann equation solver. In this preliminary study, the homogenous graphene sheet is chosen as the system-under-simulation.

The structure of the paper is as follows: In Section II, the simulation framework is briefly explained. The DC simulation results are shown in Section III. The transient simulation results are presented in Section IV. Finally, conclusions are made in Section V.

II. SIMULATION FRAMEWORK

Let us consider a phase space, (\mathbf{r}, \mathbf{k}) , where \mathbf{r} is the position vector and \mathbf{k} is the momentum vector. The Boltzmann transport equation reads:

$$\frac{\partial f}{\partial t} + Lf = S\{f\}, \quad (1)$$

where $f(\mathbf{r}, \mathbf{k}, t)$ is the distribution function, L is the free-streaming operator, and $S\{f\}$ is the scattering integral. The free-streaming operator contains the partial derivatives with respect to the position and momentum:

$$Lf = \mathbf{v} \cdot \nabla_{\mathbf{r}} f + \frac{1}{\hbar} \mathbf{F} \cdot \nabla_{\mathbf{k}} f, \quad (2)$$

where \mathbf{v} is the group velocity, \hbar is the reduced Planck constant, and \mathbf{F} is the force. The force is calculated from the electric field.

Note that the phase space is usually re-written in a way to show the kinetic-energy, ε , explicitly [14]. For example, in the case of the two-dimensional momentum space, the phase space is written as $(\mathbf{r}, \varepsilon, \theta)$. θ is an angle variable in the kinetic energy space, which is a function of \mathbf{k} . In the kinetic-energy-based representation, the free-streaming operator in (2) is written as

$$Lf_{\varepsilon}(\mathbf{r}, \varepsilon, \theta, t) = \mathbf{v} \cdot \nabla_{\mathbf{r}} f_{\varepsilon} + \mathbf{F} \cdot \mathbf{v} \frac{\partial f_{\varepsilon}}{\partial \varepsilon} + \frac{1}{\hbar} \mathbf{F} \cdot (\nabla_{\mathbf{k}} \theta) \frac{\partial f_{\varepsilon}}{\partial \theta}, \quad (3)$$

where f_{ε} is the distribution function in the kinetic-energy-based representation. The second term in the right-hand side is related with the partial derivative with respect to the kinetic energy. It is proportional to the force.

As discussed in [5], the deterministic Boltzmann equation solvers have been mainly employed for the steady-state simulation. The primary reason is the existence of a strong electric field inside the device. When the electric field is strong, the second term in (3) plays a significant role. Without a proper numerical treatment, combination of two partial derivative terms – first two terms in (3) – introduces a numerical instability

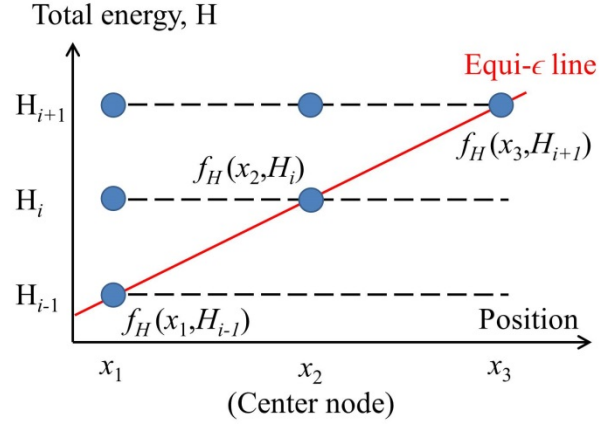


Fig. 1. Three-point discretization method for the transient simulation of a homogeneous system. Dots represent the discretized points.

[14].

In order to eliminate the numerical instability, the H-transformation [15] has been proposed. The kinetic energy variable is transformed to the total energy variable, H . In this case, the free-streaming operator is written as

$$Lf_H(\mathbf{r}, H, \theta, t) = \mathbf{v} \cdot \nabla_{\mathbf{r}} f_H + \frac{1}{\hbar} \mathbf{F} \cdot (\nabla_{\mathbf{k}} \theta) \frac{\partial f_H}{\partial \theta}, \quad (4)$$

where f_H is the distribution function in the total-energy-based representation and the gradient in the real space must be carried out consistently in that representation. Since the partial derivative with respect to the kinetic energy disappears completely, the numerical stability of the solver is greatly improved. For nanoscale devices with a strong electric field, the H-transformation seems to be mandatory for any practical simulation.

When applied to the transient simulation, however, the H-transformation introduces a serious difficulty. Since the electrostatic potential changes as the time elapses, the time derivative in the total-energy-based representation contains an additional term. In the two-dimensional momentum space, the time derivative reads:

$$\frac{\partial f_{\varepsilon}(\mathbf{r}, \varepsilon, \theta, t)}{\partial t} = \frac{\partial f_H(\mathbf{r}, H, \theta, t)}{\partial t} - q \frac{\partial \phi}{\partial t} \frac{\partial f_H(\mathbf{r}, H, \theta, t)}{\partial H}, \quad (5)$$

where q is the elementary charge and ϕ is the electrostatic potential. Therefore, when the electrostatic

potential is time-varying, the partial derivative with respect to the total energy appears again. It degrades the numerical stability of the solver significantly.

Development of a general scheme for the transient simulation, while keeping the H-transformation, would be beyond the scope of this paper. Fortunately, as much as we consider homogeneous systems like graphene sheets, we can set the electrostatic potential freely. Using this observation, a three-point discretization method is used in this work as shown in Fig. 1. The center node is surrounded by two neighboring nodes (left and right ones). When the applied electric field is time-varying, the distances between the center node and the neighboring nodes are adjusted in such a way that the potential difference between two adjacent nodes is exactly matched to the energy spacing,

$$\mathbf{x}_2 - \mathbf{x}_1 = \mathbf{x}_3 - \mathbf{x}_2 = \frac{\Delta H}{qE_x}, \quad (6)$$

where ΔH is the uniform energy spacing. Using this trick, no interpolation of the distribution function is required, because the following relations are satisfied:

$$\begin{aligned} f_H(\mathbf{x}_2, H, t) &= f_H(\mathbf{x}_1, H - \Delta H, t) \\ &= f_H(\mathbf{x}_3, H + \Delta H, t). \end{aligned} \quad (7)$$

Moreover, at the center node, the electrostatic potential itself is fixed. Therefore, the second term in (5) is eliminated. As a result, the time derivative becomes much simpler,

$$\frac{\partial f_\varepsilon(\mathbf{x}_2, \varepsilon, t)}{\partial t} = \frac{\partial f_H(\mathbf{x}_2, H, t)}{\partial t}, \quad (8)$$

which is helpful for implementing the transient simulation capability.

III. DC SIMULATION

Our in-house deterministic Boltzmann equation solver for the graphene sheet [16] has been extended to simulate the transient response. In this Section, for the sake of readability, a general description about the solver and the physical models is reproduced briefly.

The Boltzmann equation solver is based on the Fourier

harmonics expansion [1]. In this expansion, angle-dependent transport parameters (such as the density-of-states, the scattering rate, and the distribution function) are expanded with Fourier harmonics. The H-transformation is adopted as a stabilizing scheme. The three-point discretization method shown in Section II is used.

An n-type sample is considered. The linear dispersion relation of the graphene sheet is assumed. For an electron whose momentum is given by \mathbf{k} , its kinetic energy, ε_k , is given by

$$\varepsilon_k = \hbar v_F |\mathbf{k}|, \quad (9)$$

where \hbar is the reduced Planck constant. The Fermi velocity (v_F) of 10^6 m sec⁻¹ is used.

The intrinsic phonon scatterings (intravalley acoustic phonons, optical phonons, and intervalley acoustic phonons) are included in the simulation. In addition to those intrinsic phonon scatterings, the remote phonon scattering is also included in order to consider the impact of the substrate. The transition rate from \mathbf{k} to \mathbf{k}' , $S(\mathbf{k}'|\mathbf{k})$, is given by

$$\begin{aligned} S(\mathbf{k}'|\mathbf{k}) &= A_\pm \frac{\exp(-2qd)}{2(\epsilon(q))^2 q} (1 + \cos\theta) \\ &\times \delta(\varepsilon_{k'} - \varepsilon_k \pm \hbar\omega) \end{aligned} \quad (10)$$

where A_\pm is a proportional coefficient, $\mathbf{q} = |\mathbf{k}' - \mathbf{k}|$ is the momentum transfer, d is the distance between the graphene layer and the substrate, $\epsilon(\mathbf{q})$ is the dielectric function, θ is the angle difference, $\hbar\omega$ is the phonon energy, and $\delta(\cdot)$ is the Dirac delta function. The upper sign is for the phonon absorption, while the lower one is for the phonon emission. Since the remote phonon scattering is anisotropic, its transition rate is calculated directly by numerical integration. For this purpose, the angle variable, θ , is uniformly discretized. The number of discretized points for the angle variable is denoted as N_θ .

Model parameters for above-mentioned scattering mechanisms are taken from [17] and [18] without modification.

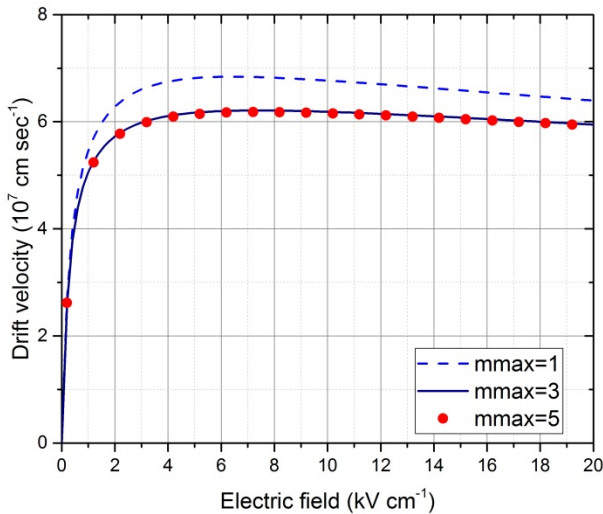


Fig. 2. Drift velocity as a function of the applied electric field for electron density of $5 \times 10^{11} \text{ cm}^{-2}$. The monolayer graphene on the SiO_2 substrate is assumed.

Fig. 2 shows the drift velocity of the graphene on the SiO_2 substrate as a function of the applied electric field. The electron sheet density is $5 \times 10^{11} \text{ cm}^{-2}$. Due to high mobility of the graphene sheet, the drift velocity rapidly increases at low-field regime. The maximum velocity is about $6 \times 10^7 \text{ cm sec}^{-1}$. Impact of the maximum order of Fourier harmonics (m_{max}) is tested. When m_{max} is 1, the drift velocity is overestimated. However, already with $m_{\text{max}} = 3$, an accurate result is obtained. It has been found that the drift velocity does not change for the tested values of N_{theta} (10, 20, and 40). The difference between $N_{\text{theta}} = 10$ and $N_{\text{theta}} = 20$ is around 0.01 %.

IV. TRANSIENT SIMULATION

In this Section, the transient response of graphene sheets on the SiO_2 substrate is simulated. Values of m_{max} and N_{theta} are 3 and 10, respectively.

For the time discretization, the backward Euler method is used. In order to minimize the numerical damping due to the coarse time step, 100 time points are simulated for every period.

First, the ac mobility of the graphene sheet is calculated. Instead of relying on the small-signal analysis, the full transient simulation has been performed and the simulated results are collected. A sufficiently long simulation (10 periods) has been performed for each case in order to eliminate the effect of initial transient behavior. Two DC operating points, 1 kV cm^{-1} and

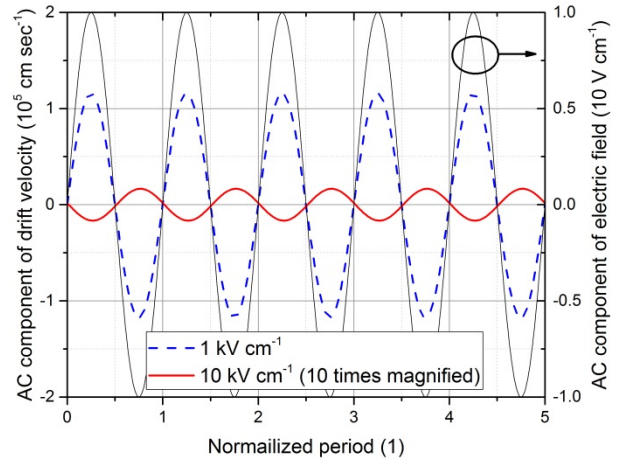


Fig. 3. AC component of the drift velocity as a function of the normalized period. Only the first five periods are shown for clarity. Two DC operating points are considered. The excitation frequency is 10 GHz.

10 kV cm^{-1} , are selected. Note that a negative differential mobility is observed at 10 kV cm^{-1} , as shown in Fig. 2. The amplitude of sinusoidal excitation is kept as a small value of 10 V cm^{-1} .

Fig. 3 shows the AC component of the drift velocity as a function of the normalized period. The excitation frequency is 10 GHz, which is sufficiently low. At 1 kV cm^{-1} , the AC drift velocity is almost in-phase with the sinusoidal excitation. However, at 10 kV cm^{-1} , the AC drift velocity is 180° out of phase. It is due to the negative differential mobility. In both cases, the simulated amplitudes are well matched to the ones calculated from the DC results shown in Fig. 2.

Fig. 4 shows the frequency dependence of the AC drift velocity. The DC electric field is 10 kV cm^{-1} . When the excitation frequency is increased to 1 THz, the amplitude of the AC drift velocity is also increased and the phase shift is clearly observed. For even higher frequency (10 THz), the amplitude of the AC drift velocity drops again. Note that such a behavior is not observed for near-equilibrium cases.

Fig. 5 shows the magnitude of AC mobility as a function of the excitation frequency. At 10 kV cm^{-1} , the AC mobility clearly shows its maximum value around 2 THz.

Next, the step response of the graphene sheet is calculated. To see the large-signal effect, the electric field is increased from 10 V cm^{-1} (which is almost negligible) to 10 kV cm^{-1} linearly. Various ramping speeds have been tested. Fig. 6 shows the drift velocity

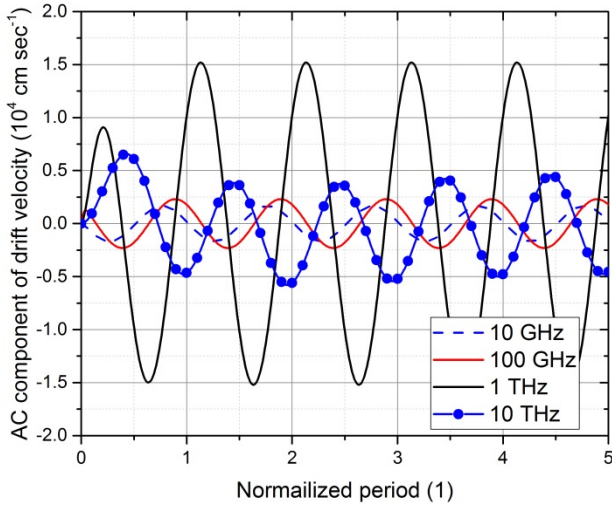


Fig. 4. AC component of the drift velocity at 10 kV cm^{-1} as a function of the normalized period. Four excitation frequencies (10 GHz, 100 GHz, 1 THz, and 10 THz) are considered.

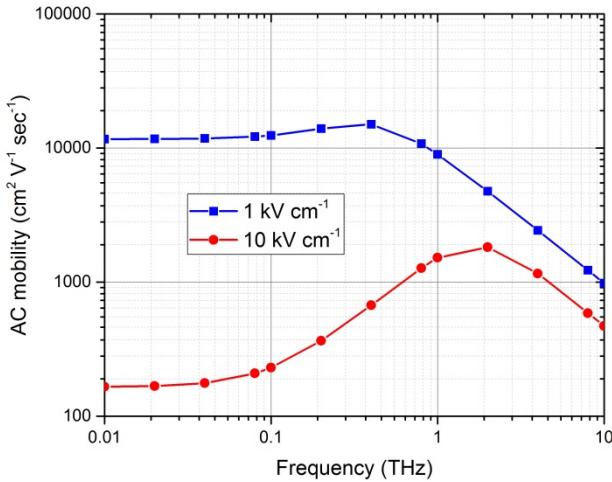


Fig. 5. Magnitude of AC mobility as a function of the excitation frequency.

as a function of normalized time. The time is normalized using the duration of ramping period. For slow ramping, the quasi-static behavior is clearly observed. However, for faster ramping, the strong non-quasistatic response is obtained. Especially for cases with ramping period shorter than 10 psec, strong velocity overshoot is observed.

Direct extension of the proposed discretization scheme to the general device simulation seems to be difficult due to the time-varying potential inside the device. Introduction of a certain interpolation scheme for the distribution function is unavoidable. The numerical properties of the transient simulation will heavily depend

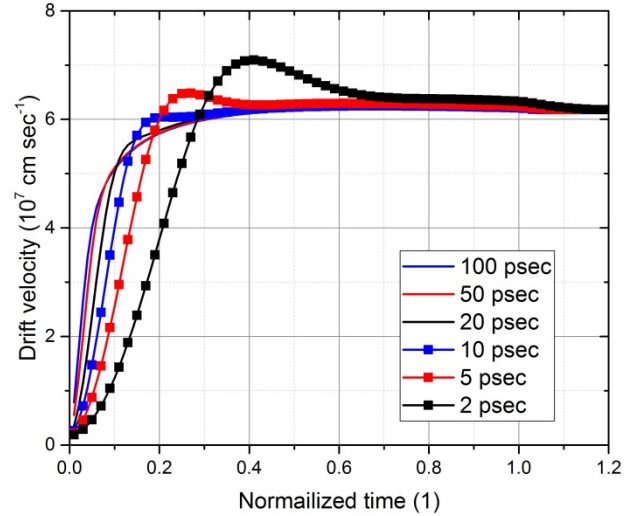


Fig. 6. Step response of the drift velocity as a function of normalized time. For each case, duration of ramping period is used as the normalization constant.

on the quality of interpolation scheme.

VI. CONCLUSIONS

In order to perform the transient simulation using a deterministic Boltzmann equation solver, it is required to treat the time derivative properly. It has been shown that simulation of homogeneous systems can be done without abandoning the H-transformation, as much as a specially designed discretization method is employed. According to the proposed method, neither the time derivative nor the free-streaming operator couples two nodes with different H-values. As examples, the AC mobility and step response of the graphene sheet have been calculated.

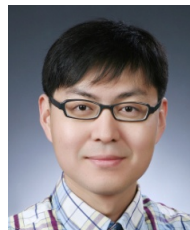
ACKNOWLEDGMENTS

This work was supported by the Samsung Research Funding Center of Samsung Electronics under Grant SRFC-IT1401-08.

REFERENCES

- [1] S.-M. Hong, A.-T. Pham, and C. Jungemann, *Deterministic Solvers for the Boltzmann Transport Equation*, Springer Verlag Wien/New York, 2011.
- [2] S.-M. Hong and C. Jungemann, "A fully coupled scheme for a Boltzmann-Poisson equation solver

- based on a spherical harmonics expansion,” *Journal of Computational Electronics*, vol. 8, pp. 225-241, 2009.
- [3] C. Jungemann, “A deterministic approach to RF noise in silicon devices based on the Langevin Boltzmann equation,” *IEEE Transactions on Electron Devices*, vol. 54, pp. 1185-1192, 2007.
- [4] D. Ruic and C. Jungemann, “Numerical aspects of noise simulation in MOSFETs by a Langevin-Boltzmann solver,” *Journal of Computational Electronics*, vol. 14, pp. 21-36, 2015.
- [5] K. Rupp, C. Jungemann, S.-M. Hong, B. Bina, T. Grasser, and J. Jüngel, “A review on recent advances in the spherical harmonics expansion method for semiconductor device simulation,” *Journal of Computation Electronics*, vol. 15, pp. 939-958, 2016.
- [6] M. Dyakonov and M. Shur, “Shallow water analogy for a ballistic field effect transistor: New mechanism of plasma wave generation by dc current,” *Physical Review Letters*, vol. 71, pp. 2465-2468, 1993.
- [7] S. Bhardwaj, N. K. Nahar, S. Rajan, and J. L. Volakis, “Numerical analysis of terahertz emissions from an ungated HEMT using full-wave hydrodynamic model,” *IEEE Transactions on Electron Devices*, vol. 63, pp. 990-996, 2016.
- [8] S. Di, K. Zhao, T. Lu, G. Du, and X. Liu, “Investigation of transient responses of nanoscale transistors by deterministic solution of the time-dependent BTE,” *Journal of Computational Electronics*, vol. 15, pp. 770-777, 2016.
- [9] Y. Cheng, I. M. Gamba, A. Majorana, and C.-W. Shu, “Discontinuous Galerkin solver for the semiconductor Boltzmann equation,” *International Conference on Simulation of Semiconductor Processes and Devices*, pp. 257-260, 2007.
- [10] Y. Koseki, V. Ryzhii, T. Otsuji, V. V. Popov, and A. Satou, “Giant plasmon instability in dual-grating-gate graphene field-effect transistor,” *Physical Review B*, vol. 93, p. 245408, 2016.
- [11] S.-M. Hong, “Transient device simulation using a deterministic Boltzmann equation solver,” *Asia-Pacific Workshop on Fundamentals and Applications of Advanced Semiconductor Devices*, pp. 185-188, 2016.
- [12] Y.-M. Lin, K. Jenkins, D. Farmer, A. Valdes-Garcia, P. Avouris, C.-Y. Sung, H.-Y. Chiu, and B. Ek, “Development of graphene FETs for high frequency electronics,” *International Electron Device Meeting*, pp. 237-240, 2009.
- [13] M. G. Ancona, “Electron transport in graphene from a diffusion-drift perspective,” *IEEE Transactions on Electron Devices*, vol. 57, pp. 681-689, 2010.
- [14] C. Jungemann, A. T. Pham, B. Meinerzhagen, C. Ringhofer, and M. Böllhofer, “Stable discretization of the Boltzmann equation based on spherical harmonics, box integration, and a maximum entropy dissipation principle,” *Journal of Applied Physics*, vol. 100, p. 024502, 2006.
- [15] A. Gnudi, D. Ventura, G. Baccarani, and F. Odeh, “Two-dimensional MOSFET simulation by means of a multidimensional spherical harmonics expansion of the Boltzmann transport equation,” *Solid-State Electronics*, vol. 36, pp. 575-581, 1993.
- [16] S.-M. Hong and S. Cha, “Deterministic Boltzmann equation solver for graphene sheets including self-heating effects,” *International Conference on Simulation of Semiconductor Processes and Devices*, pp. 197-200, 2016.
- [17] K. M. Borysenko, J. T. Mullen, E. A. Barry, S. Paul, Y. G. Semenov, J. M. Zavada, M. Buongiorno Nardelli, and K. W. Kim, “First-principles analysis of electron-phonon interactions in graphene,” *Physical Review B*, vol. 81, p. 121412, 2010.
- [18] R. Rengle, C. Couso, and M. J. Martín, “A Monte Carlo study of electron transport in suspended monolayer graphene,” *Spanish Conference on Electron Devices*, pp. 175-178, 2013.



Sung-Min Hong (M’08) received the B.S. degree in electrical engineering and the Ph.D. degree in electrical engineering and computer science from Seoul National University, Seoul, Korea, in 2001 and 2007, respectively. He is currently an

Assistant Professor with the School of Information and Communications, Gwangju Institute of Science and Technology, Gwangju, Korea. His current research interests include deterministic Boltzmann equation solvers and simulation of terahertz devices.